

Study of the proton-proton collisions at 1683 MeV/c

K. N. Ermakov, V. A. Nikonov, O. V. Rogachevsky, A. V. Sarantsev, V. V. Sarantsev, and S. G. Sherman

Petersburg Nuclear Physics Institute NRC KI, Gatchina 188300, Russia

Received: date / Revised version: date

Abstract. The new data on the elastic pp and single pion production reaction $pp \rightarrow pn\pi^+$ taken at the incident proton momentum 1683 MeV/c are presented. The data on the $pp \rightarrow pn\pi^+$ reaction are compared with predictions from the OPE model. To extract contributions of the leading partial waves the single pion production data are analyzed in the framework of the event-by-event maximum likelihood method together with the data measured earlier. The analysis allows us to obtain the assessment with a better precision the contributions from different initial partial waves.

PACS. 13.75.Cs Nucleon-nucleon interactions – 13.85.Lg Total cross sections – 25.40.Ep Inelastic proton scattering

1 Introduction

Understanding the proton-proton interactions at low and intermediate energies is one of the important tasks of the particles physics. At large momentum transfers where the strong coupling is small, the QCD calculations can be used efficiently for the description of such processes. A large progress was made at low energies where the effective field approach allowed us to describe the processes below the resonance region. However the region of the intermediate energies and especially the region of the resonance production is much less accessible for theoretical calculations and phenomenological dynamic models play here a leading role. The data from the NN collision reactions forms the basis for the construction of such models which, in turn, have a large range of applications in the nuclear and heavy ion physics.

In the region above two pion production threshold up to 1 GeV the $NN \rightarrow \pi NN$ reaction is dominated by the production of the $\Delta(1232)$ isobar in the intermediate state. It is natural to suggest that such production is based on the one pion exchange mechanism (OPE) and set of the corresponding models were put forward [1, 2, 3] a rather long time ago. The pion exchange amplitudes are introduced there using a certain form factors with parameters defined from the fit of experimental data. The model of Suslenko et al. describes with a reasonable accuracy (up to normalization factors) the differential spectra of the $pp \rightarrow pn\pi^+$ and $pp \rightarrow pp\pi^0$ reactions in the energy range below 1 GeV [2, 4], while the model of Dmitriev et al. was applied to the energy region over 1 GeV [3]. In the more complicated model based on the one boson exchange mechanism [5] the dominant contribution for the $\Delta(1232)$

production is also defined by the one pion exchange: it was found that other boson exchanges contribute around 10% to the total cross section at the energies above 1 GeV. However it should be noted that the discrepancies between the measured total cross sections and the OPE model predictions [2] are rather sizeable (see Ref. [4]). Moreover in the region above incident proton momentum 1.5 GeV/c other contributions start to play a notable role: for example a relatively broad Roper resonance is traced in the spectrum. Therefore for the comprehensive analysis of the data it is necessary to apply an approach beyond the OPE model.

With this purpose we perform the partial wave analysis of the data on the single pion production in the framework of the approach based on the work [6]. The result of the such analysis for the lower energy data sets obtained earlier was reported in [7], [8].

In the analysis [8] some solutions were found which almost equally described the data. These solutions differ by the contribution from the partial waves with the high orbital momentum $L > 3$ which were found to be rather unstable in the fit. It is interesting to compare which solution will be compatible with the present higher energy data. It is also interesting to compare the results of the partial wave analysis with the ones predicted by the OPE model.

In this paper, we present the new data on the elastic and the $pp \rightarrow pn\pi^+$ reactions measured at the momentum 1683 MeV/c. We compare the data with OPE model calculations and determine the contributions of different partial waves from the combined partial wave analysis of the present data and the data measured earlier.

Correspondence to: saran@pnpi.spb.ru

Table 1. Numbers of events and the total cross sections at the beam momentum 1683 MeV/c. The total elastic cross section was obtained by the interpolation of the differential cross section by the Legendre polynomials.

$pp \rightarrow$	events	σ mb
elastic	2772	23.96 ± 0.57
$pn\pi^+$	2564	18.97 ± 0.57
$d\pi^+$	57	0.42 ± 0.05
$d\pi^+\pi^0$	7	0.05 ± 0.02

2 The experiment. Elastic scattering

The description of the experiment performed at the PNPI 1 GeV synchrocyclotron was given in details in our previous work [7]. The proton beam was formed by three bending magnets and by eight quadrupole lenses. The mean incident proton momentum value was inspected by the kinematics of the elastic scattering events. The accuracy of the incident momentum value and momentum spread was about 0.5 MeV/c and 10 MeV/c (FWHM) correspondingly. A total of 8×10^4 stereoframes were obtained. The frames were double scanned to search for events due to an interaction of the incident beam. The double scanning efficiency was determined to be 99.95%. Approximately 7×10^3 two-prong events were used for subsequent analysis.

The 2-prong events selected in the fiducial volume of the hydrogen bubble chamber were geometrically reconstructed and kinematically fitted to the following reaction hypotheses:

$$p + p \rightarrow p + p, \quad (1)$$

$$p + p \rightarrow p + n + \pi^+, \quad (2)$$

$$p + p \rightarrow p + p + \pi^0, \quad (3)$$

$$p + p \rightarrow d + \pi^+, \quad (4)$$

$$p + p \rightarrow d + \pi^+ + \pi^0. \quad (5)$$

The events identification procedure was also described in details in [7]. Thus, we list only the most severe criteria here:

1. Events with the confidence level of more than 1% were accepted.
2. Events with only one acceptable hypothesis were identified as belonging to this hypothesis.
3. If several versions revealed a good χ^2 value, we used the visual estimation of the bubble density of the track to distinguish between a proton (deuteron) and a pion.

The total number of 2-prong events which had not passed the reconstruction and fitting procedures was counted to be less than 10%. These unidentified events were apportioned to the fraction of the fitted hypotheses of accepted events and were used only for the total cross sections calculations.

The standard bubble chamber procedure [4] was used to obtain absolute cross sections for the elastic and pion production reactions. The precision of the determination

of the millibarn-equivalent was 2%. The values of the cross sections for inelastic processes together with statistics of the events selected by the fit are listed in Table 1. Let us remind that data on the $pp \rightarrow pp\pi^0$ reaction at the same energy were published earlier [9].

The differential cross section for the elastic pp scattering measured in the present experiment is shown in Fig. 1 as open squares with statistical errors. There is a notable loss (not shown in Fig. 1) of the very forward events when a slow proton had a short recoil path and could not be seen in the bubble chamber or was missed during the scanning. In Fig. 1 we compare our elastic differential cross section with the data from the EDDA experiment [10] taken at the incident momentum 1687.5 MeV/c (open red circles). One can see that there is a good agreement between our points and the EDDA data, that supports the correctness of our definition of the millibarn-equivalent.

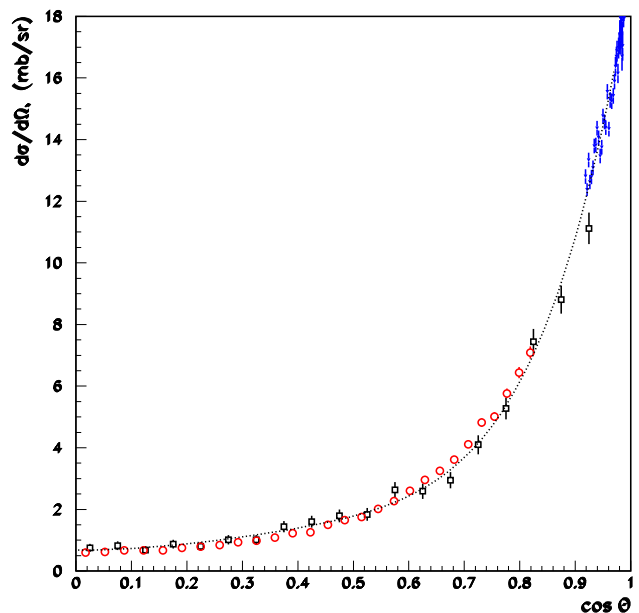


Fig. 1. (Color online) Elastic differential cross section. The dotted curve is result of the Legendre polynomial fit of our data (open squares) restricted by the interval $0 \leq \cos \theta \leq 0.95$ and the data from [11] (blue triangles). The open red circles show the measurements of the EDDA experiment [10] taken at the incident momentum 1687.5 MeV/c.

To obtain the total elastic cross section we applied the following procedure. To take above losses into account we fitted the differential cross section with a sum of even order Legendre polynomials $A_n P_n(\cos \theta)$ $n = 0, 2, 4, \dots$. By examining the behavior of the Legendre coefficients with decrease of the fitted angular range we determined the range $0 \leq \cos \theta < 0.95$ as unbiased one. So the last experimental point at $\cos \theta > 0.95$ was not included in the further fit because we do not know the real amendment for it. For finding of the total elastic cross section we included in the fit above $\cos \theta = 0.95$ the data from [11] at the incident momentum 1685.7 MeV/c which provide an important constraint for high order polynomials. The re-

sult of the fit is shown in Fig. 1 as the dotted curve. The total elastic cross section calculated as $2\pi A_0$ was found to be 23.96 ± 0.57 mb which is close to the value given in [12].

3 The $pp \rightarrow pn\pi^+$ reaction and a comparison with the OPE model

The OPE model [2] describes the single pion production reactions by four pole diagrams with the π^0 or π^+ exchanges (we should like to express the deep appreciation to the authors [2] for the accordance of their program code). In this model the intermediate state of the πN -scattering amplitude confines itself to the P_{33} wave only, assuming the leading role of the Δ_{33} -resonance.

The Fig. 2 shows the distributions over the momentum transfer squared, $\Delta^2 = -(p_t - p_f)^2$, where p_t is the four-momentum of the target proton and p_f is the four-momentum of the final proton or neutron in the $pp \rightarrow pn\pi^+$ reaction correspondingly. The OPE model calculations normalized to the total number of the experimental events is shown by the dashed lines and the shape of the phase volume is shown with the dotted lines. One can see that the OPE model describes qualitatively well the Δ^2 distributions for the studied reaction.

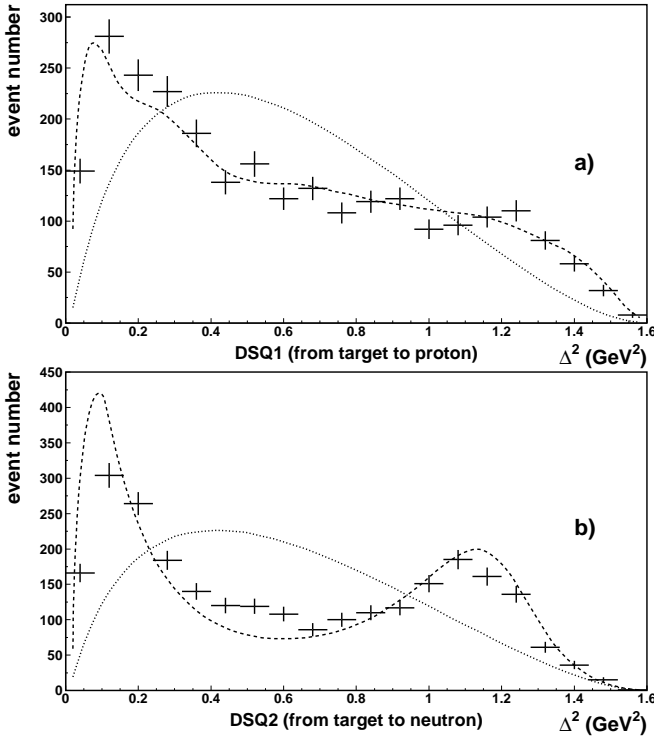


Fig. 2. Four-momentum transfer Δ^2 distribution for the $pp \rightarrow pn\pi^+$ reaction: a) for the transfer to the final proton and b) to neutron. The dashed curves are the OPE calculations and the dotted curves show the shape of the phase space.

Fig. 3 presents the c.m.s. angular distributions, effective two-particle mass spectra of the final particles and the angular distributions in the helicity frames.

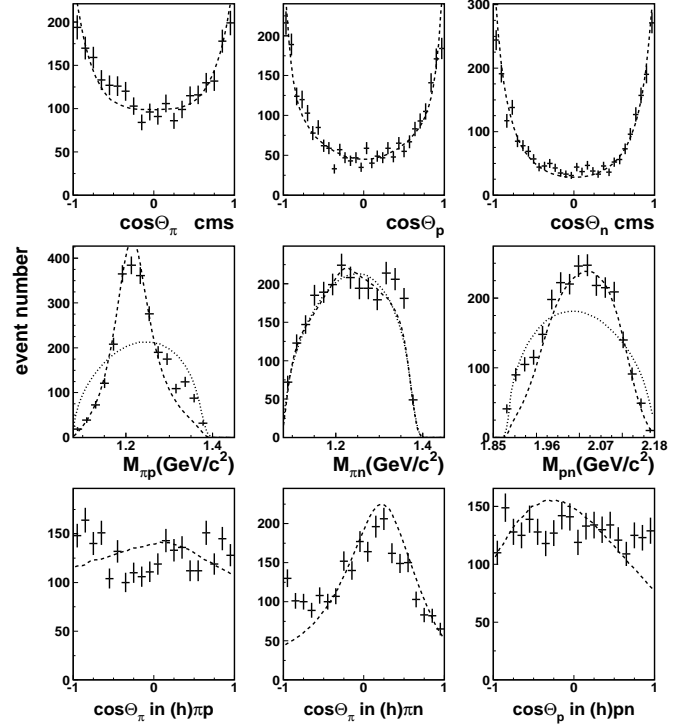


Fig. 3. The $pp \rightarrow pn\pi^+$ data (the crosses with statistic errors): angular distributions of the final particles in the c.m.s. of the reaction (upper line), the effective two-particle mass spectra (middle line) and angular distributions in the helicity systems. The dashed curves show the OPE calculations and dotted curves show the shape of the phase space

It is seen that the calculations of the OPE model normalized to the total number of the experimental events reproduce the particle angular distributions in the c.m.s. of the reactions and the two body mass spectra fairly well. However the angular distributions in the helicity systems show a notable deviations from the experimental points.

4 Formalism of the partial wave analysis

The partial wave analysis was performed in the framework of the event-by-event maximum likelihood method. The formalism is given in details in [6, 13] and based on the spin-orbital momentum decomposition of the initial and final partial wave amplitudes. Therefore it is natural to use the spectroscopic notation $^{2S+1}L_J$ for the two particle partial wave with the intrinsic spin S , the orbital momentum L and the total spin J . Here and below we use S, L, J for the description of an initial NN system, S_2, L_2, J_2 for a system of two final particles and $S', L', J' = J$ for a system formed by the two-final particle system and the spectator.

The total amplitude can be written as a sum of partial wave amplitudes as follows [6, 13]:

$$A = \sum_{\alpha} A_{tr}^{\alpha}(s) Q_{\mu_1 \dots \mu_J}^{in}(SLJ) A_{2body}^{S_2, L_2, J_2}(s_i) \times Q_{\mu_1 \dots \mu_J}^{fin}(i, S_2 L_2 J_2 S' L' J), \quad (6)$$

where $Q(S, L, J)$ are operators which describe a system with the intrinsic spin S , the orbital momentum L and the total spin J . A_{tr}^{α} is the transition amplitude and $A_{2body}^{S_2, L_2, J_2}$ describes rescattering processes in the intermediate two-particle channel. Multy-index α includes all quantum numbers for the description of the definite partial wave, s is the invariant energy of the initial NN system squared and s_i is the invariant energy squared of the two-particle system.

To suppress contributions of amplitudes at high relative momenta we introduced the Blatt-Weisskopf form factors. Thus the energy dependent part of the partial wave amplitudes with production of a resonance, for example, in the two-particle system 12 (e.g. πp) and the spectator particle 3 (n) has the form:

$$A = \frac{A_{tr}^{\alpha} A_{2body}^{S_2, L_2, J_2}(s_{12}) q^L k_3^{L'}}{\sqrt{F(q^2, L, R) F(k_3^2, L', r_3)}}, \quad (7)$$

where q is the momentum of the incident proton and k_3 is the momentum of the spectator particle, both calculated in c.m.s. of the reaction. The explicit form of the Blatt-Weisskopf form factors $F(k^2, L, r)$ can be found, for example, in [13]. One should expect that the effective radius of the initial proton-proton system R should vary between $1 \div 4$ fm. However, due to a relatively large distance from the pp threshold it is hard to expect that this value can be determined with a good accuracy in the present analysis. Indeed we did not observe any sensitivity to this parameter and fixed it at 1.2 fm. A very similar result was observed for r_3 . So for our final fits we also fixed this parameter at 1.2 fm.

The combined analysis of the data sets at different energies allows us to extract the energy dependence of the partial waves which is assumed to be a smooth function in this energy interval. In the fit it was introduced in the following form:

$$A_{tr}^{\alpha}(s) = \frac{a_1^{\alpha} + a_3^{\alpha} \sqrt{s}}{s - a_4^{\alpha}} e^{ia_2^{\alpha}}, \quad (8)$$

where a_i^{α} are real parameters. The a_4^{α} parameters define poles located in the region of left-hand side singularities of the partial wave amplitudes. Such poles are usually a good approximation of the left-hand side cuts defined by the boson exchange diagrams. The phases a_2^{α} are defined by contributions from logarithmic singularities connected with three body rescattering in the final state.

For the description of the energy dependence in the πN system we introduce two resonances: $\Delta(1232)_{\frac{3}{2}}^{+}$ and Roper $N(1440)_{\frac{1}{2}}^{+}$. The corresponding amplitudes are parameterized as follows:

$$A_{2body}^{S_2, L_2, J_2}(s_{12}) = \frac{k_{12}^{L_2}}{\sqrt{F(k_{12}^2, L_2, r_{12})}} \frac{1}{M_R^2 - s_{12} - M_R \Gamma},$$

$$\Gamma = \Gamma_R \frac{M_R k_{12}^{2L_2+1} F(k_R^2, L_2, r_{12})}{\sqrt{s_{12}} k_R^{2L_2+1} F(k_{12}^2, L_2, r_{12})}. \quad (9)$$

Here s_{12} is the invariant energy squared in the channel 12, k_{12} is the relative momentum of particles 1 and 2 in their rest frame and r_{12} is the effective radius.

For $\Delta(1232)$, we use M_R and Γ_R taken from PDG [14] with $r_{12} = 0.8$ fm. The Roper state was parameterized using couplings found in the analysis [15] where decays of this state into the πN , $\Delta\pi$ and $N(\pi\pi)_{S-wave}$ channels were determined.

For the description of the final NN interaction we use the following parameterization:

$$A_{2body}^{S_2, L_2, J_2}(s_{23}) = \frac{\sqrt{s_{23}}}{1 - \frac{1}{2} r_{23}^{\beta} k_{23}^2 a^{\beta} + i k_{23} a^{\beta} \frac{k_{23}^{2L_2}}{F(k_{23}^2, r_{23}^{\beta}, L_2)}}. \quad (10)$$

For the S -waves it coincides with the scattering-length approximation formula suggested in [16, 17]. Thus the parameter a^{β} can be considered as the NN -scattering length and r^{β} is the effective range of the NN system.

5 Partial wave analysis results and discussion

We performed the analysis of new data starting from our solution obtained in [8]. This solution was restricted by the partial waves with the total spin J up to 2 and the orbital momentum L up to 3. This solution which produced an acceptable description of a lower energy data showed a notable problems for the new data set. For example, the χ^2 for the normalized angular distribution of the neutron in the c.m.s. of the reaction is equal to 4.49. The main problem is seen in the description of the extreme angles which are most sensitive to partial waves with high orbital momentum. Indeed, the solution with $L \leq 5$ and $J \leq 4$ found in [8] (but only used for the error estimation in that paper) predicts the χ^2 to be 1.23. The description of the data with these two solutions is shown in Fig. 4. This provides a strong argument for the presence of higher partial waves at studied energy.

Although the solution with $L \leq 5$ produced a rather good description of the normalized differential cross section, the total cross section predicted from both solutions appeared to be about 10% lower then that given by the data. Therefore we used the last solution as a starting point and performed the combined fit of the present data together with the $pp \rightarrow pp\pi^0$ data measured earlier [4, 9, 18] and the $pp \rightarrow pn\pi^+$ data taken at 1628 and 1581 MeV/c [7, 8].

On this way we were able to reproduce both the differential and the total cross sections for all fitted data with a good accuracy. The results of the partial wave analysis are shown in Fig. 5: the histograms correspond to the Monte Carlo events weighted by the differential cross section calculated from the fit parameters. The χ^2 for distributions shown in this Figure is varied from 0.65 (for the pion angular distribution in the c.m.s. of the reaction) to 2.6 (for the πp invariant mass). We would like to remind that we

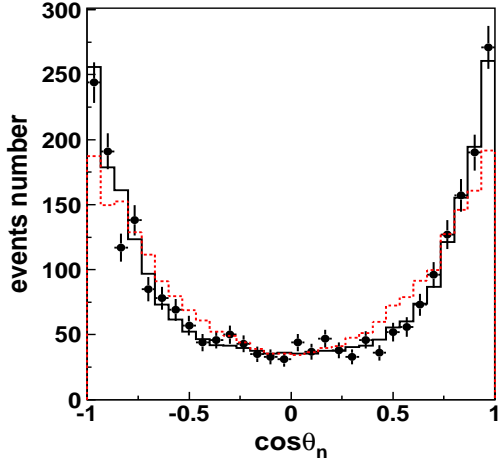


Fig. 4. (Color online) The neutron angular distribution calculated in the c.m.s. of the $pp \rightarrow pn\pi^+$ reactions at 1683 MeV/c. The data are shown by black circles with statistical errors. The solid (black) histogram shows the prediction from the solution [8] with including partial waves up to $L = 3$ and the dotted (red) one the prediction from the solution with L up to 5.

use the event-by-event maximum likelihood analysis and do not fit directly these distributions.

The partial wave analysis reproduces rather well the helicity distributions which have systematic deviations for the OPE model predictions. The OPE model calculations normalized to the $\Delta(1232)$ production contributions calculated from the partial wave analysis are shown in Fig. 5 as dashed lines for the angular distributions in the helicity systems. It is seen that $\Delta(1232)$ production from the partial wave analysis and from the OPE model corresponds well each to another. This confirms that $\Delta(1232)$ is produced by the one pion exchange mechanism and the deviation of the data from the OPE model is due to the production of the Roper state.

The present combined analysis found the contributions from the leading initial partial waves to be in a qualitative agreement with the prediction from the solution reported in [8]. However we observe changes for the contributions of the initial partial waves 1D_2 and 3F_2 which are notably increased after the fit of the new data. As concern the partial waves with total spin $J = 4$ we found a sizeable contribution from 3F_4 .

For all initial partial waves the contribution of channels with the $\Delta(1232)$ production varies from 65 to 100% and only for the 3P_0 wave it was found to be rather small one: 12%. The Roper resonance is produced mostly (in the decreasing order of contributions) from the 3P_2 , 3P_0 , 3P_1 states and by one order smaller from 1S_0 . We found a notable contribution for the decay of the initial 3P_2 state to the (pn) subsystem 1P_1 with isospin $I = 0$.

To study the stability of the solution we added to the fit the partial waves with the total spin J up to 5 decaying into $\Delta(1232)N$. Such solutions demonstrated some reduction of the contribution from the 3P_0 initial state and increasing the contributions from the 3F_2 state. Taking into account these ambiguities we have performed an

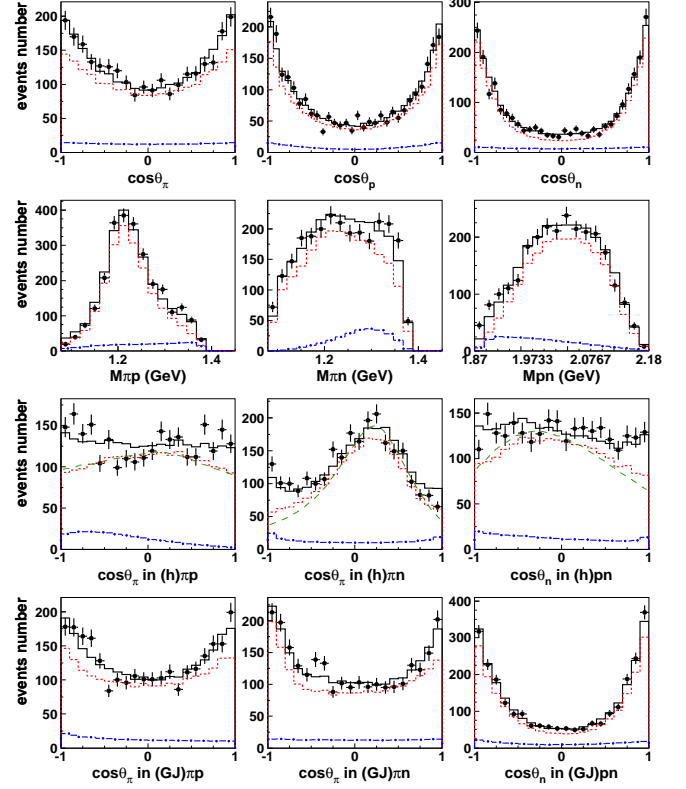


Fig. 5. (Color online) The $pp \rightarrow pn\pi^+$ data taken at the proton momentum 1683 MeV/c with statistic errors only. First line: the angular distributions of the final particles in the c.m.s. of the reaction. Second line: the effective two-particle mass spectra. Third line: the angular distributions of the final particles in the helicity frames. Fourth line: the angular distributions in the final particles in the Gottfried-Jackson frame. The solid (black) histograms show the result of our partial wave analysis; the dotted (red) and dot-dashed (blue) histograms show the contributions from the production of the $\Delta(1232)$ and $N(1440)$ intermediate states. The dashed (green) curves in the helicity frame show the normalized distributions from the OPE model.

error analysis of the initial state contributions to the single pion production cross sections. For the $pp \rightarrow pn\pi^+$ reaction these contributions are shown for three incident momenta in Fig. 6.

It is necessary to mention that the present combined analysis defines contributions of the partial waves with better errors than it was found in [8]: this is mostly influenced by the solutions with high spin amplitudes included and the interference of waves with the Roper production in πN and non-resonant pn systems.

The obtained solution is well compatible with the HADES data on the single pion production at 1.25 GeV [19]: including these data in the combined fit does not change the main results of the analysis.

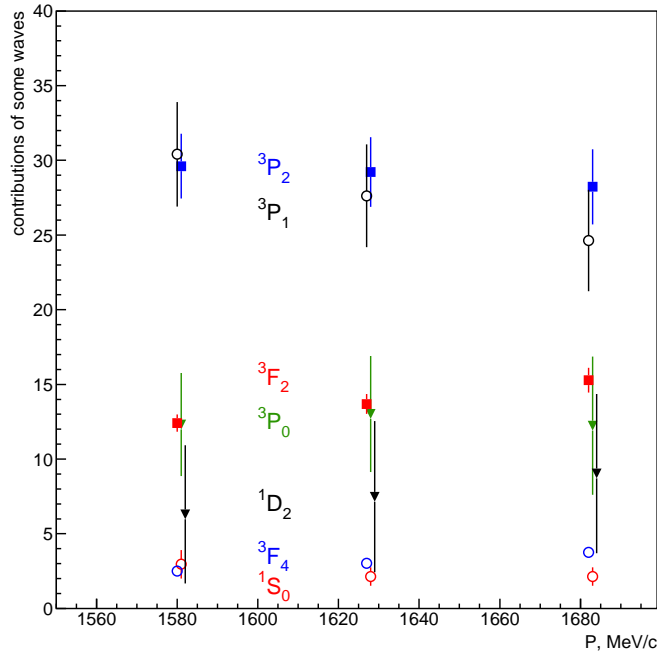


Fig. 6. (Color online) Contributions (the percentages) of most important waves in the $pp \rightarrow pn\pi^+$ reaction

6 Conclusion

The new data on the elastic and $pp \rightarrow pn\pi^+$ reactions taken at the incident proton momentum 1683 MeV/c are reported. Including these inelastic data in the combined partial wave analysis of the single pion production reactions leads to a better error analysis and therefore to a more precise definition of the partial wave contributions to the $pp \rightarrow pn\pi^+$ reaction. We observe some changes and in specific transition amplitudes compare to the predictions from the solution [8].

As noted earlier in Ref. [4], although the OPE model provides a qualitative description of most differential spectra, it disagrees with the total cross section values for the $pp \rightarrow pp\pi^0$ and $pp \rightarrow pn\pi^+$ reactions. However our partial wave analysis confirms that the $\Delta(1232)$ production is defined by the OPE exchange mechanism and the difference is due to the production of the Roper state.

The all analyzed data sets can be downloaded from the Bonn-Gatchina data base [20] as 4-vectors and directly used in the partial wave analysis by other groups. We would like to remind that although we supply a Monte Carlo sample in our web page one can use a standard sample of the 4π generated events: the bubble chamber events have efficiency close to 100%.

We would like to express our deep gratitude to the bubble chamber staff as well as to laboratory assistants, which toiled at the film scanning and measuring. The work of V.A.Nikonov and A.V.Sarantsev is supported by the RNF grant 16-12-10267.

References

1. E. Ferrari and F. Selleri, *Nuovo Cimento* **27**, 1450 (1963).
2. V. K. Suslenko and I. I. Gaisak, *Sov. J. Nucl. Phys.* **43**, 252 (1986) [*Yad. Fiz.* **43**, 392 (1986)].
3. V. Dmitriev *et al.*, *Nucl.Phys.* **A459**, 503 (1986).
4. V. P. Andreev *et al.*, *Phys. Rev. C* **50**, 15 (1994).
5. A. Engel *et al.*, *Nucl.Phys.* **A603**, 387 (1996).
6. A. V. Anisovich *et al.*, *Eur. Phys. J. A* **34**, 129 (2007).
7. K. N. Ermakov *et al.*, *Eur. Phys. J. A* **47**, 159 (2011).
8. K. N. Ermakov *et al.*, *Eur. Phys. J. A* **50**, 98 (2014).
9. V. V. Sarantsev *et al.*, *Eur. Phys. J. A* **21**, 303 (2004).
10. D. Albers *et al.*, *Eur. Phys. J. A* **22**, 125 (2004).
11. A. V. Dobrovolsky *et al.*, *Nucl. Phys. B* **214**, 1 (1987).
12. F. Shimizu *et al.*, *Nucl. Phys.* **A386**, 571 (1982).
13. A. V. Anisovich and A. V. Sarantsev, *Eur. Phys. J. A* **30**, 427 (2006).
14. J. Beringer *et al.* [Particle Data Group Collaboration], *Phys. Rev. D* **86**, 010001 (2012).
15. A. V. Anisovich *et al.*, *Eur. Phys. J. A* **48**, 15 (2012).
16. K. M. Watson, *Phys. Rev.* **88**, 1163 (1952).
17. A. B. Migdal, *JETP* **1**, 2 (1955).
18. S. A. El-Samad *et al.* [COSY-TOF Collaboration], *Eur. Phys. J. A* **30**, 443 (2006).
19. G. Agakishiev *et al.* [HADES Collaboration], *Eur. Phys. J. A* **51**, no. 10, 137 (2015). doi:10.1140/epja/i2015-15137-5
20. Bonn-Gatchina PWA group: pwa.hiskp.uni-bonn.de